

Multiplicative and Additive Modulation of Neuronal Tuning with Population Activity Affects Encoded Information

Highlights

- Neuronal tuning in macaque V1 is modulated by fluctuations in population activity
- Modulation involves multiplicative and additive effects
- Neurons with strong multiplicative effects have weak additive effects and vice versa
- Encoded information in neuronal ensembles depends on the type of modulation

Authors

Iñigo Arandia-Romero, Seiji Tanabe, Jan Drugowitsch, Adam Kohn, Rubén Moreno-Bote

Correspondence

ruben.moreno@upf.edu

In Brief

Arandia-Romero et al. show that neuronal tuning is modulated with fluctuations in population activity, increasing the information provided by multiplicatively modulated neurons and decreasing that provided by additively modulated neurons. Population activity thus determines which neurons are most informative.

Multiplicative and Additive Modulation of Neuronal Tuning with Population Activity Affects Encoded Information

Iñigo Arandia-Romero,^{1,2} Seiji Tanabe,³ Jan Drugowitsch,⁴ Adam Kohn,³ and Rubén Moreno-Bote^{1,2,5,6,*}

¹Department of Information and Communication Technologies, Universidad Pompeu Fabra, Barcelona 08018, Spain

²Research Unit, Parc Sanitari Sant Joan de Deu, Esplugues de Llobregat, Barcelona 08950, Spain

³Dominick Purpura Department of Neuroscience and Ophthalmology and Visual Science, Albert Einstein College of Medicine, Bronx, NY 10461, USA

⁴Département des Neurosciences Fondamentales, Université de Genève, 1211 Geneva 4, Switzerland

⁵Centro de Investigación Biomédica en Red de Salud Mental (CIBERSAM), Esplugues de Llobregat, Barcelona 08950, Spain

⁶Serra Hünter Fellow Programme, Universidad Pompeu Fabra, Barcelona 08018, Spain

*Correspondence: ruben.moreno@upf.edu

<http://dx.doi.org/10.1016/j.neuron.2016.01.044>

SUMMARY

Numerous studies have shown that neuronal responses are modulated by stimulus properties and also by the state of the local network. However, little is known about how activity fluctuations of neuronal populations modulate the sensory tuning of cells and affect their encoded information. We found that fluctuations in ongoing and stimulus-evoked population activity in primate visual cortex modulate the tuning of neurons in a multiplicative and additive manner. While distributed on a continuum, neurons with stronger multiplicative effects tended to have less additive modulation and vice versa. The information encoded by multiplicatively modulated neurons increased with greater population activity, while that of additively modulated neurons decreased. These effects offset each other so that population activity had little effect on total information. Our results thus suggest that intrinsic activity fluctuations may act as a “traffic light” that determines which subset of neurons is most informative.

INTRODUCTION

Neuronal activity fluctuates at both the single-neuron and the population levels. These activity fluctuations can limit the reliability of neuronal codes because a given response can arise from several distinct sensory stimuli (Shadlen and Newsome, 1998; Tolhurst et al., 1983). Fluctuations in stimulus-evoked responses have been generally viewed as harmful noise that needs to be averaged out to extract the desired signal (Cohen and Maunsell, 2009; Mitchell et al., 2009; Shadlen and Newsome, 1998; Averbach et al., 2006). Recent work has shown, however, that population activity fluctuations modulate single-cell stimulus-evoked responses in additive and multiplicative manners (Ecker et al., 2014; Goris et al., 2014; Lin et al., 2015; Schölvinck

et al., 2015), suggesting that they are highly structured and hence might have a computational role. Nevertheless, the role, if any, of fluctuations of total activity in neuronal populations on sensory neuronal tuning and encoding has not been demonstrated.

We studied the influence of population activity fluctuations on the responses of single neurons and small neuronal ensembles in primary visual cortex (V1) of both anesthetized and awake monkeys. We found that the tuning for stimulus orientation of orientation-selective neurons changes multiplicatively or additively with the total, stimulus-evoked activity of the neuronal population that embeds these individual neurons, while leaving their tuning width and orientation preference mostly unaffected. While distributed on a continuum, neurons with strong multiplicative effects tended to have weak additive effects and vice versa, suggesting some specificity of the modulation across neurons. Consistent with a multi-gain model of neuronal responses, we found that neurons and small neuronal ensembles with strong multiplicative effects became more informative with stronger population activity, whereas those with strong additive effects became less informative. Population activity before stimulus onset was also predictive of both tuning modulation and changes in encoded information, but to a lesser degree than stimulus-evoked population activity. Importantly, we found that population activity does not substantially alter total sensory information in the recorded population. Rather, it routes how this information is represented, in an antagonist way, into multiplicatively and additively modulated neurons and neuronal ensembles. These results suggest that intrinsic fluctuations in the activity of neuronal populations may act as a “traffic light” that modulates the tuning of individual neurons and can differentially redistribute sensory information in the neuronal population.

RESULTS

We recorded neuronal populations in the superficial layers of V1 in four anesthetized (datasets 1–4, D1–D4) and one awake (D5) macaque monkeys. We measured responses to gratings drifting in 8 (12 for D5) equally spaced directions. Gratings were presented for 1,280 ms (350 ms) each, interleaved with a 1,500-ms

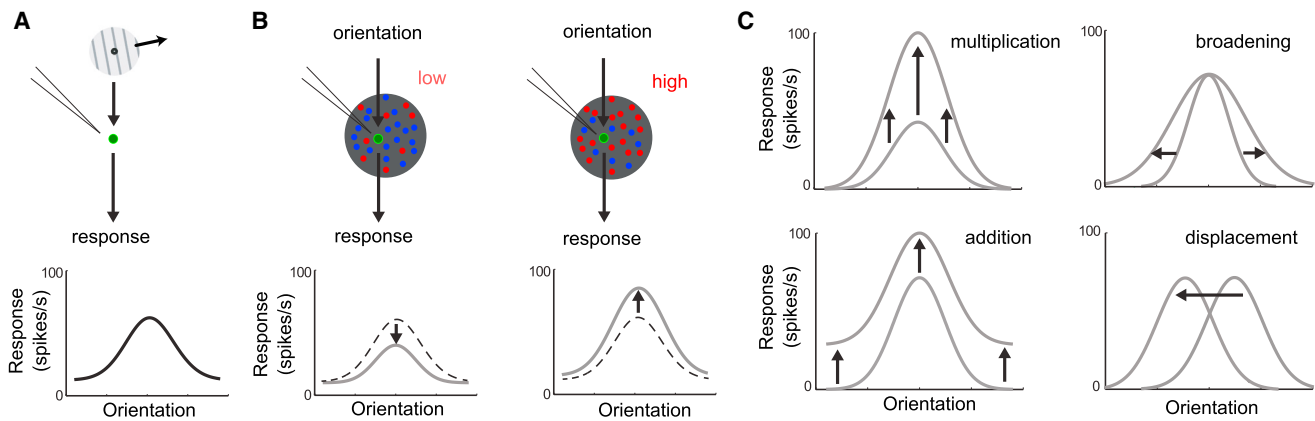


Figure 1. Hypothetical Modulation of Sensory Tuning with Population Activity

(A) The “classical” tuning of a neuron, computed without conditioning on population activity.

(B) The firing rate of the neuron can depend on population activity. When population activity is low, tuning could have a lower gain (gray line, left); when population activity is high, tuning might have a higher gain (right). If the activity of the neuron is independent of population activity, the tuning for the two cases would be identical to the “classical” tuning (dashed lines).

(C) Tuning can be modulated in several ways with fluctuations in population activity, including multiplicative and additive effects, or both, and broadening and displacement.

(50 ms) blank screen and repeated 300 or 400 (50) times in random order. We analyzed the activity of 567 single neurons and multiunits, which we refer to together as “units.” We studied 122, 106, 73, 161, and 18 simultaneously recorded units in datasets D1 to D5, respectively. We also analyzed separately a subset of 83 well-isolated single neurons (27, 14, 7, 31, and 4 from D1–D5, of which 12, 12, 4, 15, 2, were orientation selective; see [Experimental Procedures](#)).

The firing rate of many V1 neurons is tuned to the orientation of a drifting grating (illustrated in [Figure 1A](#)). Since neurons are embedded in a local network and are correlated (median of pairwise spike count correlations: $\rho = 0.21$ across all anesthetized datasets), the summed total activity of that local population (called population activity) might modulate this tuning ([Figure 1B](#)). This modulation could involve multiplicative or additive effects, or both, as well as broadening and displacement ([Figure 1C](#)). Similarly, positive correlations among neurons can arise in multiple ways, such as additive modulation, multiplicative modulation, broadening of tuning, or a combination of these effects or others ([Figure S1A](#)). Therefore, the existence of correlations does not specify how tuning is modulated. We thus developed an analysis that could distinguish how tuning is modulated with population activity fluctuations.

In our data, population activity showed substantial fluctuations across trials for a fixed stimulus condition (several representative trials shown in [Figure 2A](#), left), consistent with previous reports ([Arieli et al., 1996](#); [Ecker et al., 2014](#); [Schölvinck et al., 2015](#)). The distribution of spike counts during the stimulation period across trials for one stimulus was roughly unimodal and broad ([Figure 2A](#), right; similar unimodal distributions were obtained in all datasets, [Figure S2A](#)). We characterized the timescale of the fluctuations using the spontaneous activity periods. Fluctuations in population activity were correlated with a timescale of a few hundreds of milliseconds ([Figure S2B](#)), in consonance with other studies on single neuron activity in V1 ([Ecker et al., 2014](#);

[Kohn and Smith, 2005](#)). Population activity was negatively correlated with local field point (LFP) signals ([Figure S2C](#)), as previously reported ([Okun et al., 2015](#)).

We tested how neuronal tuning varies with fluctuations in population activity using a model-free approach by comparing responses of a single neuron when the activity of the rest of the recorded neurons was either high (defined as the half of trials in which the summed population activity was greatest) or low (remaining trials). We used all recorded units to define periods of high and low population activity, excluding the neuron whose tuning was being characterized to avoid artifacts. Therefore, any observed modulation of tuning must arise from network effects and would not be observed for uncorrelated neural populations. Both tuning and population activity were measured during the entire duration of the evoked activity period (shorter periods are considered below).

The tuning of an example single neuron depended clearly on population activity ([Figure 2B](#)): responses were stronger when population activity was high (dark red box, [Figure 2B](#)) compared with when it was low (light red). To characterize how tuning was altered, we first determined whether there was substantial broadening (where tuning width was defined as the distance between peak to half-peak) or displacement of tuning with population activity. To quantify these effects, we fit the tuning of each neuron with a von Mises function (see [Experimental Procedures](#)). Across single neurons, we found a small (2% relative change) widening of tuning when population activity was high compared with low, but this effect was not significant ([Figure S3A](#); Mann-Whitney $U = 855$, $p = 0.2$). Tuning preference was also only weakly modulated with population activity ([Figure S3B](#); median absolute displacement = 1.0 degrees; permutation test $p < 0.002$), a small shift when compared with the typical tuning width. Therefore, we conclude that changes in tuning width and preference are small and that the influence of population activity can only involve multiplicative and additive modulation of tuning.

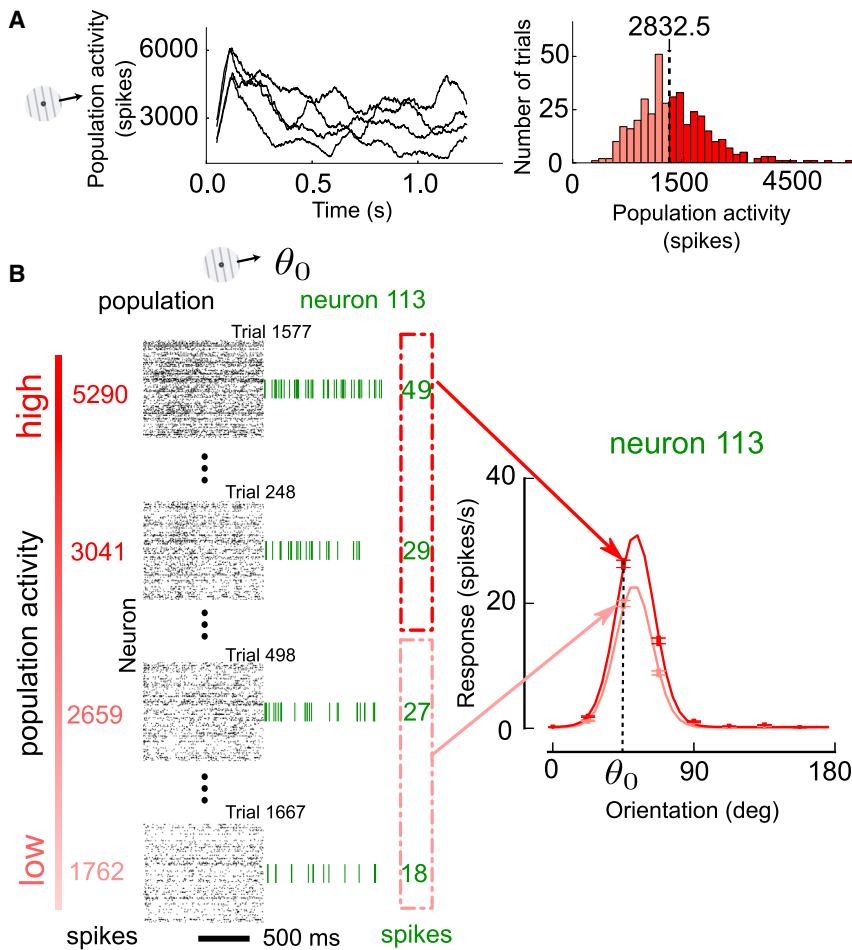


Figure 2. Sensory Tuning Depends on Population Activity in an Example Single Neuron

(A) Stimulus-evoked population activity fluctuates across trials for the same stimulus (left). Four trials are shown. Distribution of population activity (sum of spikes across all neurons in the recorded population) across trials for a given stimulus (right) is shown.

(B) The tuning of a single neuron (neuron 113 in D4) is strongly modulated with population activity (population activity is defined here as the sum of spikes across all neurons, excluding the activity from the neuron for which tuning is being characterized). Population activity was ranked from high (top left) to low (bottom left) for each stimulus orientation θ_0 . The activity of the selected neuron (green spike trains) was averaged across either the top (red box) or bottom (light red box) 50th percentile of trials, and the averages were plotted as a function of stimulus orientation (right most). The tuning was modulated with population activity (red versus pink lines), with stronger responses during periods of high population activity. Points and error bars are mean responses and SEM, respectively; lines are von Mises fits.

fit with slope larger than one that passes through the origin, whereas neurons with purely AFs will have fits with slope one and a positive intercept. In a separate analysis, we confirmed that estimates of the MFs and AFs from von Mises fits to the tuning gave similar results (data not shown).

For the example single neuron of [Figure 2B](#), tuning was modulated multiplicatively (MF = 1.4, permutation test $p < 0.002$) with little additive modulation (AF = 0.009, $p = 0.01$).

The four example neurons of [Figure 3A](#) displayed different levels of multiplicative and additive modulation. For instance, the neuron in the second panel was modulated in a mostly multiplicative manner (MF = 1.5, permutation test $p < 0.002$; AF = 0.046, $p = 0.04$), and the remaining neurons displayed a combination of multiplicative and additive effects. When we calculated tuning in more finely binned sets of trials, we observed that the modulation varied smoothly with the population activity level ([Figure S3C](#)).

Statistically significant MFs and AFs were found in a substantial fraction (25/44 for multiplication and 19/44 for addition) of orientation-selective single neurons. The median MF across all single neurons was 1.27, significantly larger than one ([Figure 3C](#), left, black; Mann-Whitney $U = 264$, $p = 10^{-10}$). This corresponds to a change of 27% in the firing rate, which occurs with a 35% increase in population activity between low-activity and high-activity trials. The median AF was also significantly larger than zero ([Figure 3C](#), right, black; median = 0.05, Mann-Whitney $U = 484$, $p = 10^{-5}$), indicating a 5% increase relative to the neuron's mean firing rate at low population activity. Importantly, we found that there was a negative correlation between the MFs and AFs across single neurons ([Figure 3D](#), black dots; $\rho = -0.48$, non-parametric bootstrap $p < 0.002$, see [Experimental Procedures](#)).

Multiplicative and Additive Modulation of Tuning with Population Activity

We sought to determine the extent to which tuning was multiplicatively and additively modulated with population activity. In the following analysis ([Figures 3A–3C](#)), both tuning and evoked population activity were measured from 160 to 260 ms after stimulus onset. This brief time period was chosen such that we could, on one hand, analyze the data from awake and anesthetized animals in the same way and, on the other hand, study the temporal dynamics of the modulatory effects of population activity. The results for other time periods are discussed further below.

Tuning varied strongly with population activity ([Figure 3A](#), four examples shown). For each single neuron, we characterized its multiplicative and additive modulation with population activity by performing linear regression on the average response to each orientation, when population activity was high compared with when it was low ([Figure 3B](#)). The slope of the linear fit indicates how tuning scales multiplicatively with population activity (termed hereafter the multiplicative factor [MF]). The intercept of the fit, on the other hand, describes the additive shift to tuning with population activity. To obtain a relative measure of the additive shift, like the MF, we defined the additive factor (AF) as the ratio between this intercept and the mean firing rate of the neuron averaged across orientations. Thus, neurons with purely MFs will feature a

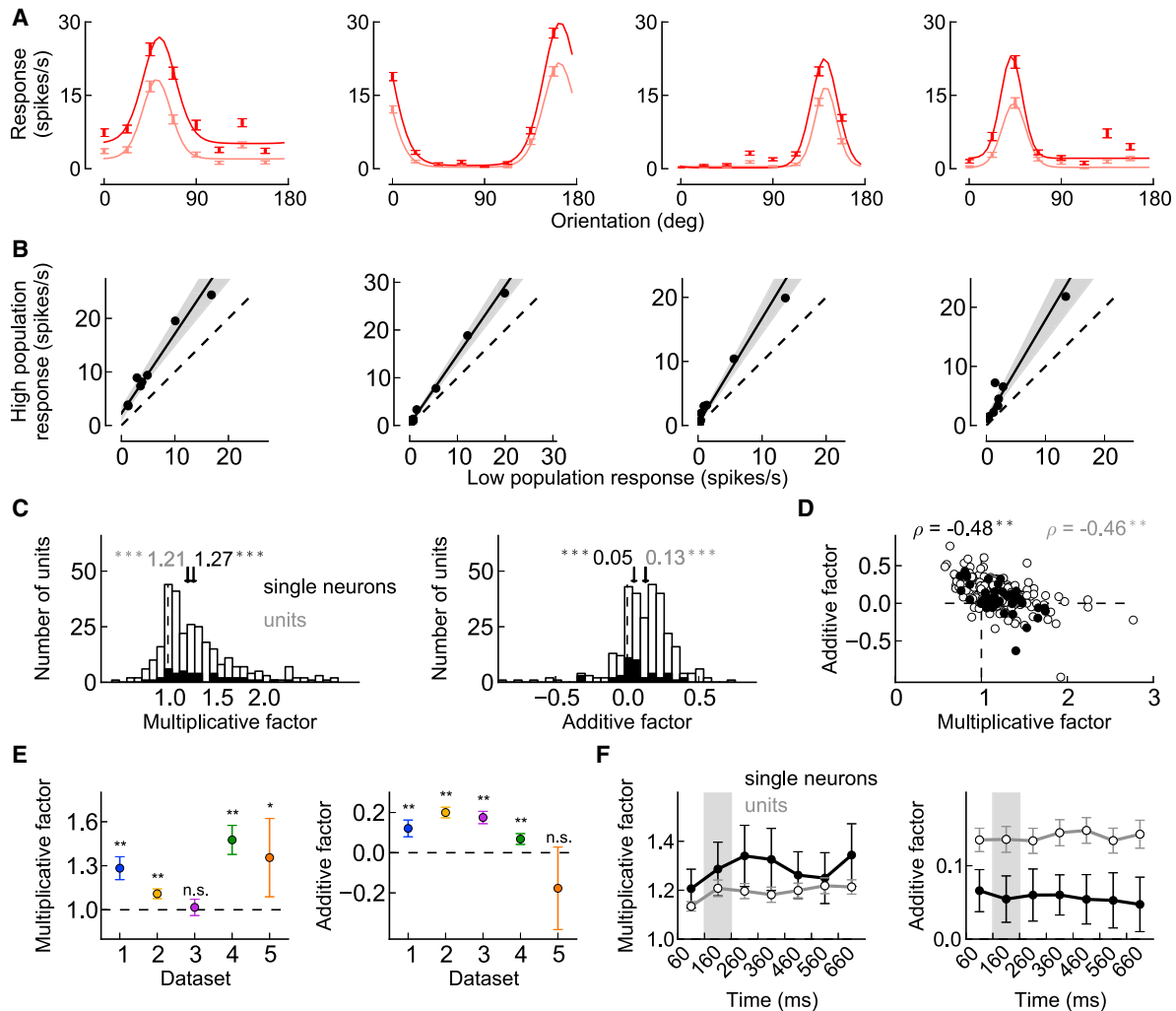


Figure 3. Sensory Tuning Undergoes Multiplicative and Additive Modulation as a Function of Population Activity

(A) Modulation of sensory tuning with population activity in four single neurons, computed as in Figure 2B. Error bars indicate SEM. (B) Mean response of single neurons when population activity is high (ordinate, corresponding to red lines in A) versus low (abscissa, light red lines in A). Each dot is the mean response to a different stimulus orientation. Shaded areas around the lines correspond to 95% confidence intervals. (C) Histograms of multiplicative (left) and additive (right) factors (MFs and AFs, respectively) for all orientation-selective single neurons (black; $N = 44$) and orientation-selective units (white; $N = 293$) for D1–D4. Median MF across single neurons is 1.27, and across units is 1.21, shown in bold and non-bold formats, respectively. Median AF across single neurons is 0.05 and across units is 0.13. (D) AFs and MFs for both single neurons (black circles) and units (open circles; all) are negatively correlated. (E) For individual datasets, MFs (left) are typically significantly larger than one. For individual datasets, AFs (right) are significantly larger than zero for all except for one dataset. (F) Median MFs and AFs as a function of time (100ms time windows), relative to stimulus onset (time zero) across single neurons (black line) and units (gray). Shaded areas indicate time window (160–260 ms) used to compute population activity and tuning curves in (A)–(E). Error bars correspond to 95% confidence intervals ($2.91 * m.a.d./\sqrt{N}$, where m.a.d. is median absolute deviation). * $p < 0.05$, ** $p < 0.01$, *** $p < 0.001$, n.s. $p > 0.05$.

The results described thus far were based on well-isolated single neurons, but remained qualitatively unchanged if we included activity from multiunits. Across all units, the median MFs and AFs were significantly larger than one and zero, respectively (Figure 3C, white; median MF = 1.21, Mann-Whitney $U = 2 \times 10^4$, $p = 10^{-48}$; median AF = 0.13, Mann-Whitney $U = 2 \times 10^5$, $p = 10^{-44}$). The negative correlation between MFs and AFs was also apparent across this large set of units (Figure 3D, white dots: $\rho = -0.46$, $p < 0.002$). Although MFs and AFs formed a con-

tinuum rather than distinct groupings, the negative correlation between MFs and AFs across both single neurons and all units indicates a partial separation of multiplicative and additive modulation with population activity.

To test whether the finding of both multiplicative and additive modulation with virtually no broadening was not due to artifacts in our estimation method, we applied the same method to simulated population activity with tuning identical to the one observed in the data (Figure S1). We created neuronal populations with

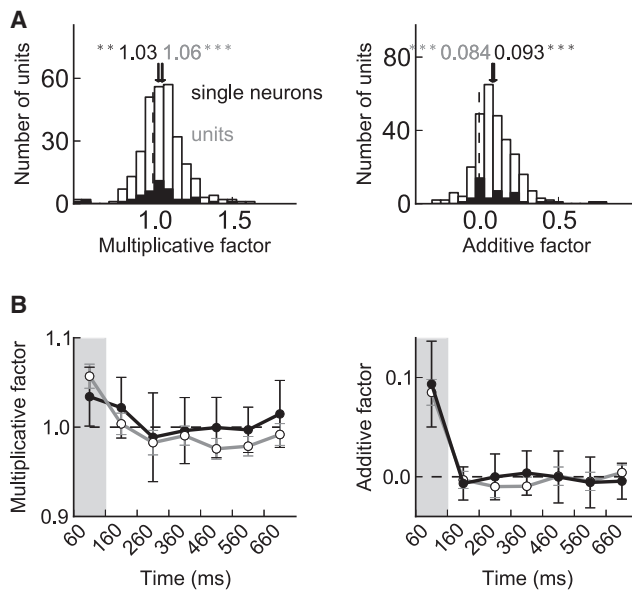


Figure 4. Sensory Tuning Depends on Pre-stimulus Population Activity

(A) Histograms of multiplicative (left) and additive (right) factors across single neurons (black) and units (white). Median MF across single neurons was 1.03 and 1.06 across units. Median AF across single neurons was 0.093 and 0.084 across units.

(B) Median MFs and AFs as a function of time (time windows of 100 ms) for single neurons (black line) and all units (gray). Shaded areas indicate time window (160–260 ms) used to compute statistics in (A), while population activity was computed during the pre-stimulus period (100 ms before stimulus onset). Error bars indicate 95% confidence intervals ($2.91 * m.a.d. / \sqrt{N}$). ** $p < 0.01$, *** $p < 0.001$.

purely multiplicative modulations, purely additive modulations, or purely broadening effects and tested whether our method discovered the true modulation while rejecting other types of modulation. The method reliably estimated the correct type of modulation in each simulated dataset (Figure S1B). We furthermore confirmed that the negative correlation between MFs and AFs found in our data was not an artifact of our estimation method, as our method could reliably detect or reject the presence of correlations between these factors in simulated data (Figure S1C).

We also evaluated the significance of modulatory factors in each dataset separately, in part to test whether there are substantial differences between anesthetized and awake preparations. We found strong and significant MFs and AFs in most individual datasets (Figure 3E). The median MFs were significant in four of five datasets, including the awake dataset (Figure 3E, right; median = 1.28, permutation test $p < 0.002$, D1; median = 1.10, $p < 0.002$, D2; median = 1.02, $p = 0.4$, D3; median = 1.48, $p < 0.002$, D4; median = 1.36, $p = 0.04$, D5). Significant positive AFs were found in all datasets (Figure 3E, right; median = 0.12, permutation test $p < 0.002$, D1; median = 0.2, permutation test $p < 0.002$, D2; median = 0.18, $p < 0.002$, D3; median = 0.07, $p < 0.002$, D4), except the awake dataset, for which there was a non-significant negative trend, presumably because of the lower

number of neurons and trials recorded when compared with the anesthetized datasets (Figure 3E, right; median = -0.18 , $p = 0.4$, D5). We also confirmed that the negative correlation between MFs and AFs was present in all anesthetized datasets separately (Figure S3D), indicating that this correlation did not emerge from aggregating data with different mean values.

Substantial multiplicative and additive effects with no broadening and a negative correlation between MFs and AFs were also observed when, instead of using direct measures of population activity, we used the projection of the population activity vector onto the first component of principal component analysis (PCA) on a trial-by-trial basis (Figures S4A and S4B). Thus, our findings are not sensitive to the specific definition of population activity used but generalize to other sensible alternative measures of population activity strength.

Finally, we tested whether the tuning modulation was also present during other response epochs than the window 160–260 ms after stimulus onset, considered above. We repeated our analyses measuring both neuron tuning and population activity in 100 ms windows spanning the range from 60 to 1,260 ms. We found that the modulation of neuronal tuning with population activity was robust in these other epochs as well (Figure 3F).

Modulation of Tuning with Pre-stimulus Population Activity

We have thus far considered how tuning changes with fluctuations in evoked population activity. These population fluctuations vary slowly under spontaneous conditions, over a timescale of hundreds of milliseconds (Figure S2B), and are well-documented (Arieli et al., 1996; Ecker et al., 2014; Fiser et al., 2004; Kenet et al., 2003; Kohn and Smith, 2005; Smith and Kohn, 2008; Tsodyks et al., 1999). Spontaneous activity fluctuations have been shown to influence subsequent evoked responses (Arieli et al., 1996; Tsodyks et al., 1999). Thus, we sought to determine how tuning during stimulus presentation varies with the strength of population activity before stimulus onset. We measured population activity in the 100 ms preceding stimulus onset and tuning from 60 to 160 ms after stimulus onset. We excluded the data of the awake preparation, as the short inter-stimulus interval (50 ms) made a reliable estimation of pre-stimulus activity impossible.

Orientation tuning depended on the strength of pre-stimulus population activity. We found significant positive MFs and AFs (Figure 4A; for single neurons, median MF = 1.03, Mann-Whitney $U = 645$, $p = 0.01$; median AF = 0.093, $U = 430$, $p = 5 \times 10^{-6}$; for all units, median MF = 1.06, $U = 3 \times 10^4$, $p = 2 \times 10^{-16}$; median AF = 0.084, $U = 2 \times 10^5$, $p = 3 \times 10^{-42}$). The modulation with pre-stimulus population activity was significantly smaller than that based on fluctuations in stimulus-evoked population activity (MFs: Wilcoxon sign-rank test, $p < 0.01$; AFs: $p < 0.01$). Furthermore, the modulation with pre-stimulus activity was most evident when tuning was measured shortly after stimulus onset (60–160 ms; Figure 4B). The factors typically declined over time, as one would expect from the spike correlation times of a few hundreds of milliseconds found in our data and usually reported for V1 (Arieli et al., 1996; Ecker et al., 2014; Fiser et al., 2004; Kenet et al., 2003; Kohn and Smith, 2005; Smith and Kohn, 2008; Tsodyks et al., 1999).

A Multi-gain Model Predicts How Tuning Modulation Affects Information Encoding

Our analysis revealed that tuning undergoes both multiplicative and additive modulation as a function of population activity and that across neurons there is a negative correlation between these two types of modulation. To what extent does this tuning modulation influence encoded sensory information? Does information depend on whether the modulation was multiplicative or additive? To address these questions, we considered an idealized model with both multiplicative and additive tuning modulations. We assumed that the mean response of a neuron in the population depends on a global modulatory factor g as

$$f_i(\theta, g) = \underbrace{g_{m,i}(g)h_i(\theta)}_{\text{multiplication}} + \underbrace{g_{a,i}(g)}_{\text{addition}} = \underbrace{(1 + \alpha_i g)h_i(\theta)}_{\text{multiplication}} + \underbrace{\beta_i g}_{\text{addition}}. \quad (\text{Equation 1})$$

The first term in the sums corresponds to the multiplicative modulation of tuning, and the second term corresponds to its additive modulation. The normalized tuning function $h_i(\theta)$ describes the tuning of the neuron with respect to the sensory variable θ , which is modulated by the neuron-specific MFs and AFs, $g_{m,i}$ and $g_{a,i}$, respectively. These factors relate to a global modulatory factor, g , linearly by $g_{m,i}(g) = 1 + \alpha_i g$ and $g_{a,i}(g) = \beta_i g$. For instance, a neuron with a purely MF corresponds to $\alpha_i > 0$ and $\beta_i = 0$. The global modulatory factor g , assumed to be shared by all neurons in the population, generates correlations between neurons. Firing of each neuron, conditioned on the global modulatory factor, is assumed to be Poisson with the rate dictated by Equation 1. This multi-gain model, with arbitrary mixtures of MFs and AFs across neurons, is a generalization of recently introduced models with purely multiplicative modulation of neuronal variance and pairwise covariance (Goris et al., 2014) or with purely additive modulation to describe state transitions in neuronal populations (Ecker et al., 2014). Our model generalizes also the recent affine model (Lin et al., 2015), which allows arbitrary AFs for each neuron but features a MF identical for all neurons. In our model, in contrast, each neuron can have a different MF α_i (see Equation 1), as our data suggest (Figure 3). Using this more complex model was justified by its ability to better predict neural activity of a holdout set than alternative models (Figure S5). Most of the models described above have not been used to make predictions about information encoding (but see Lin et al., 2015), and the predictions that have been made were not tested experimentally. The multi-gain model provides specific predictions about how sensory information in neural data should depend on the multiplicative and additive modulation of tuning, which we tested.

From our multi-gain model described in Equation 1, it is straightforward to compute its Fisher information, which is a measure of discriminability between two nearby stimulus orientations (Ma et al., 2006; Seung and Sompolinsky, 1993). Because we are interested in how neurons' information about orientation depends on population activity, we conditioned information on the global modulatory factor g , resulting in

$$I_i(\theta, g) = \frac{g_{m,i}^2(g)h_i^2(\theta)}{g_{m,i}(g)h_i(\theta) + g_{a,i}(g)}, \quad (\text{Equation 2})$$

where the prime denotes a derivative with respect to the stimulus (i.e., $h'(\theta)$ is proportional to the tuning slope). This equation captures the information provided by each neuron if there is no change in the relationship between response magnitude and variability. Consistent with this assumption, we found little difference in Fano factors between trials with low or high population activity (Figure S6). We also found similar correlations for the two sets of trials (Figure S6).

Equation 2 predicts that a neuron's information about stimulus orientation increases with multiplicative gain (as its effect is dominated by the numerator), but decreases with additive modulation (as it only appears in the denominator). Intuitively, a multiplicative modulation increases the tuning slope, and thus, information grows; in contrast, an additive modulation increases the response variance without altering slope, and thus, information decreases. For instance, the neuron in the second panel of Figure 3A had a pure multiplicative gain, and therefore, its responses to different orientations became more distinct with increasing population activity, potentially increasing the sensory information encoded. In contrast, the neuron in the first panel had also a large additive modulation, which could result in a drop in the information it encodes (since the response variance will be higher for the stronger responses). Thus, how information is affected by fluctuations in population activity will depend in part on the relative prevalence of multiplicative and additive modulation in the neuron.

The Information Encoded by Neurons Depends on the Strength of Population Activity

We tested the predictions of our model with our data. As an illustration, we first selected an orientation-selective neuron that had a strong MF (1.8, permutation test $p < 0.002$; Figure 5). The prediction of the multi-gain model is that the information encoded by this neuron about stimulus orientation should increase with population activity. As a proxy for information, we used the decoding performance (fraction of correctly predicted stimulus orientation) of a multivariate logistic regression decoder (Experimental Procedures), cross-validated on holdout trials that were not used to train the decoder. Better decoding performance corresponds to an increase in sensory information (Moreno-Bote et al., 2014). Although our decoder was trained on all orientations simultaneously, we split the performance into each orientation and obtained a separate decoding performance per orientation, as the non-uniformity of tuning curves caused some orientations to be better encoded than others. In addition, for each stimulus orientation, we split the data into trials with either high or low population activity to characterize how population activity modulated information. When performing this analysis, we measured population activity as the summed activity of all recorded units, excluding the unit (or ensemble of units, see below) for which information was computed, just as when we characterized tuning modulation. For the selected unit, decoding performance increased substantially with population activity, by 44 and 9 percentage points for the two illustrated orientations (Figure 5, top). This example shows that the sensory information encoded by neurons can vary substantially with the overall population activity.

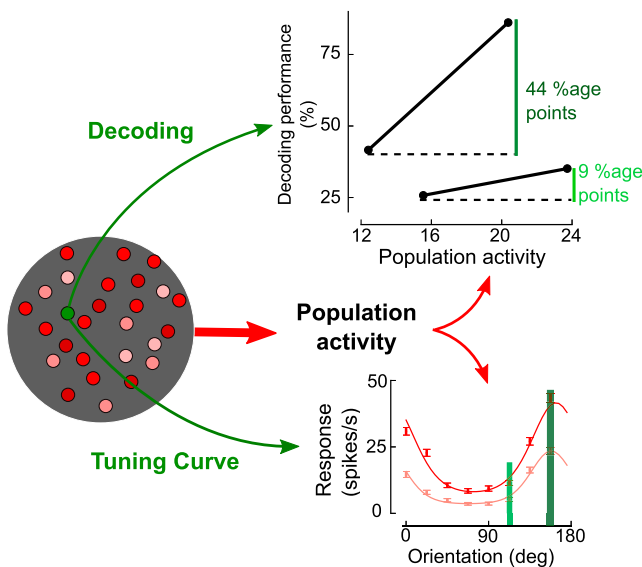


Figure 5. Information Increases with Population Activity in a Neuron with Strong Multiplicative Modulation

This unit (from D1) had a large multiplicative factor (MF = 1.8, permutation test $p < 0.002$; AF = 0.16, $p < 0.002$). Decoding performance per orientation (cross-validated probability of correctly predicting the orientation on a trial-by-trial basis) for the selected unit increases with evoked population activity for two sample orientations (top right; performance changes are indicated for the two orientations).

Sensory Information in Neuronal Ensembles

The multi-gain model predicts that neurons with stronger multiplicative effects should provide better performance with higher population activity than neurons with weaker multiplicative effects. Consistent with this prediction, we found a significant positive correlation across all units between the magnitude of the MF and the performance change when moving from low to high population activity (Figure 6A, left; $\rho = 0.6$, t test, $p < 10^{-28}$; analysis based on responses measured 160–260 ms after stimulus onset). As also predicted by the multi-gain model, units with stronger additive effects had a larger negative performance change (Figure 6A, right; $\rho = -0.32$, t test, $p = 3 \times 10^{-7}$). In summary, units with strong multiplicative effects provide more information as population activity increases, whereas units with additive modulation provide less information.

The multi-gain model also predicts that the balance of MFs and AFs should determine how the information encoded by small neuronal ensembles, not just by units, should vary with the population activity level. This is true if responses are conditionally independent given the global modulatory factor (Equation 1) such that information in the ensemble becomes the sum of the “units” contributions (Equation 2). We tested this prediction by grouping orientation-selective units, including both single neurons and multi-units, in ensembles of size N ($N = 1, 2, 3, 5, 10$ and 15) as follows. Within each dataset, we ordered orientation-selective units by their multiplicative (or additive) factors and then split them into non-overlapping ensembles of N units that preserved this ordering (Experimental Procedures). For all datasets, the correlation between performance change and average MF of

the ensemble was positive and increased rapidly for larger sizes N of the ensemble (Figure 6B, left). Examples of these correlations are shown in Figure 6C for ensembles of size $N = 5$ (except D5, where individual units are shown). The datasets from anesthetized animals featured a strong positive correlation between performance change and the average MF (Pearson’s $\rho = 0.92$, $p = 7 \times 10^{-6}$, D1; $\rho = 0.80$, $p = 4 \times 10^{-5}$, D2; $\rho = 0.87$, $p = 0.002$, D3; $\rho = 0.78$, $p = 4 \times 10^{-4}$, D4). The dataset from an awake animal (Figure 6C, last panel) showed the same trend but did not reach significance (Pearson’s $\rho = 0.66$, $p = 0.08$), most likely due to the small number of orientation-selective units available (eight neurons). On average across datasets, the performance change was roughly ten percentage points for the ensembles of $N = 5$ neurons with strongest multiplicative modulation, from a baseline performance of 44% correct (where chance performance is 12.5% in anesthetized data).

In contrast, the correlation between performance change and the average AF in the ensemble showed the opposite pattern; performance change was typically more negative for larger ensembles (Figure 6B, right). Examples of these negative correlations are shown in Figure 6D, following the same conventions as Figure 6C. In three of four anesthetized datasets, the correlation between performance change and AFs was significantly negative (Pearson’s $\rho = -0.48$, $p = 0.09$, D1; $\rho = -0.63$, $p = 0.003$, D2; $\rho = -0.97$, $p = 2 \times 10^{-5}$, D3; $\rho = -0.54$, $p = 0.03$, D4), while in the awake dataset the correlation was negative but not significant ($\rho = -0.58$, $p = 0.1$, D5). On average across datasets, the performance change was roughly -2% percentage points for the ensembles of $N = 5$ neurons with strongest additive modulation.

When, instead of using population activity, we repeated the analysis described above with the projection of the population activity vector onto the first PCA component, we again found that information was differentially modulated in ensembles with strong multiplicative and additive effects (Figures S4C–S4F). We found similar but weaker results when information in the evoked response was conditioned on the strength of population activity measure just before stimulus onset (Figure S7), consistent with the modulation of tuning with pre-stimulus activity described in Figure 4.

Population Activity Does Not Substantially Change Total Information, but Redirects Information into Additively and Multiplicatively Modulated Neuronal Ensembles

Thus far, we have shown that information increases for multiplicatively modulated ensembles and decreases for additively modulated ensembles, when population activity is stronger. But what is the net dependence of information on the strength of population activity? To address this question, we randomly selected units to form neuronal ensembles of varying sizes ($N = 1, 2, 3, 5, 10$, and 15), instead of choosing subsets of neurons based on their modulation as we did previously. We computed the performance change between low and high population activity, averaged across many ensembles. We found that there was little change in performance on average (Figure 7A, black line). However, when we selected from these randomly generated ensembles the 10% of cases with the strongest overall multiplicative modulation, we found that

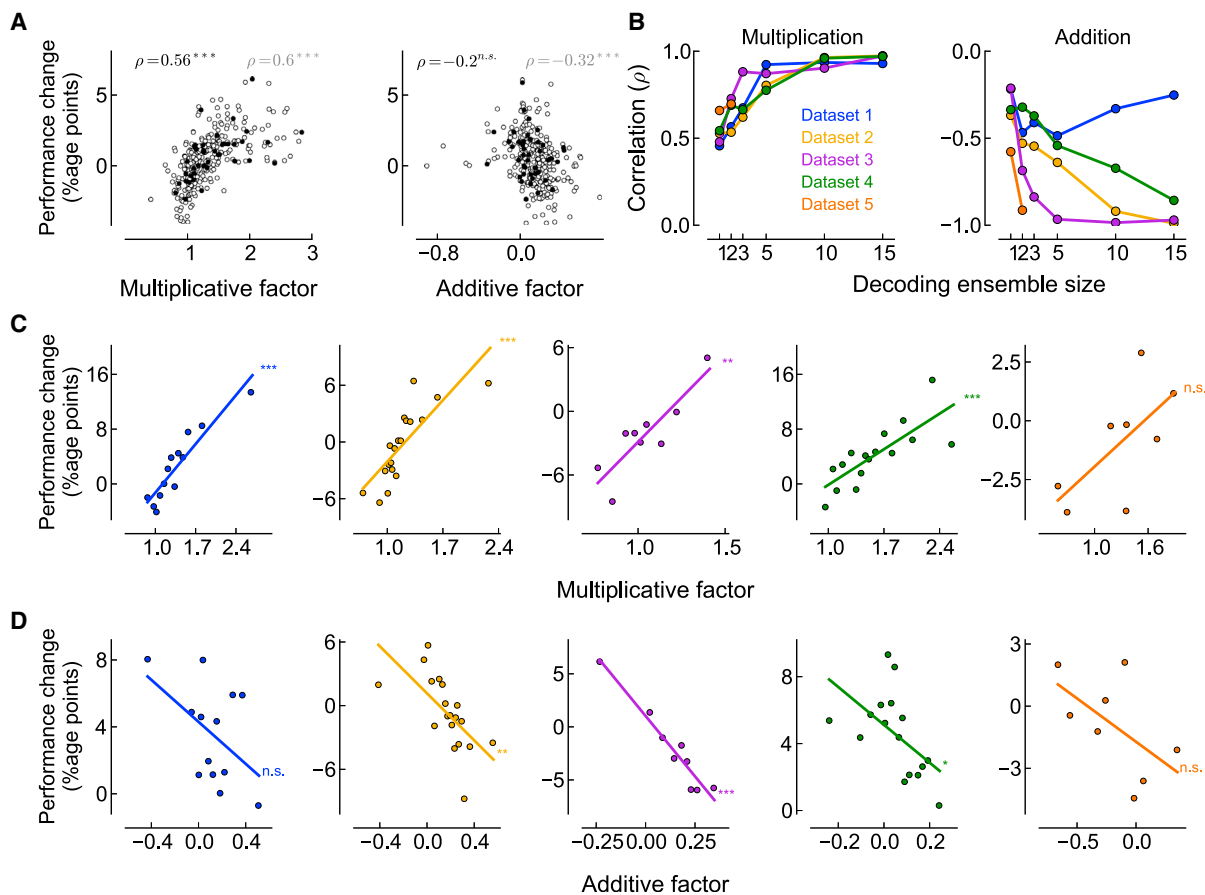


Figure 6. Performance Change Increases for Units and Ensembles of Units with Strong Multiplicative Modulation and Decreases for Those with Strong Additive Modulation when Population Activity Is Higher

(A) Performance change as a function of multiplicative (left) and additive (right) factors for all orientation-selective single neurons (black circles) and units (open circles; all).

(B) Correlation between performance change and MFs (left) or AFs (right), as a function of the number of units N in the ensemble for each dataset (same color code as in Figure 3E). Decoding is based on the entire ensemble, and the MFs and AFs refer to the average factors in the ensemble. Population activity was measured after excluding the ensemble used to decode stimulus orientation. The correlation between performance change and average MF in the ensemble increases with ensemble size and then asymptotes. In contrast, the correlation between performance change and average AF drops with ensemble size, as predicted by the multi-gain model.

(C) Performance change increases with the strength of multiplicative modulation for each dataset individually (ensembles of $N = 5$, except $N = 1$ for D5).

(D) Performance change decreases with the average AF of the ensemble (same sizes as C) and can even become negative. Significance of Pearson's correlation: * $p < 0.05$, ** $p < 0.01$, *** $p < 0.001$, n.s. $p > 0.05$.

performance change was large and saturated as a function of ensemble size (green line), consistent with our previous analysis. Similarly, when we selected the 10% of ensembles with the strongest additive modulation, we found that performance change was consistently negative (blue line).

These results suggest that in randomly sampled neuronal ensembles, the effect of population activity on information is negligible. In fact, when we computed decoding performance in these populations at low and high population activity we did not find a visible modulation (Figure 7B; the two lines overlay). Therefore, population activity does not substantially modulate the information present in these populations, but rather it modulates which ensembles have more information about the stimulus at different times. When population activity is high, the information encoded by multiplicatively modulated ensembles is enhanced; when

population activity is low, the information provided by additively modulated ensembles is more important.

DISCUSSION

We found that intrinsic fluctuations of stimulus-evoked and ongoing population activity are associated with multiplicative and additive modulation of the tuning of orientation-selective neurons in monkey V1. Neurons that showed strong multiplicative modulation tended to display weak additive modulation and vice versa. These forms of modulation affected the sensory information encoded by neurons and small neuronal ensembles. As predicted by a multi-gain model, we found that sensory information increased with population activity for neuronal ensembles with strong multiplicative gains. However, sensory

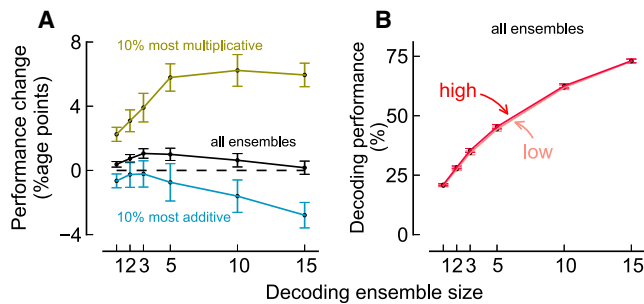


Figure 7. Population Activity Does Not Substantially Change Total Information, but Rather It Differentially Redirects Information into Multiplicatively and Additively Modulated Neuronal Ensembles

(A) Change in decoding performance averaged across randomly chosen ensembles of varying size (solid line) and for the top 10% ensembles with strongest average multiplicative (green) and additive (blue) factors. (B) Lack of modulation of performance with population activity as a function of ensemble size for randomly chosen ensembles. Error bars indicate SEM.

information decreased with greater population activity for ensembles with strong additive modulation. Importantly, we found that these effects largely offset each other so that intrinsic fluctuations of population activity do not strongly affect total sensory information. Rather, the strength of population activity seems to act as a “traffic light” that differentially redirects information into different subsets of neurons.

Previous work (Arieli et al., 1996; Tsodyks et al., 1999) found that pre-stimulus ongoing population activity has an additive effect on evoked responses, and others have reported either additive (Ecker et al., 2014) or multiplicative (Goris et al., 2014) modulations of evoked responses with population activity fluctuations. Recent work has shown that both multiplicative and additive modulations are present in mice and cat neuronal populations (Lin et al., 2015) and reported that a model with a single MF across all neurons and different AFs is favored. Instead, by observing how population activity affects tuning curves, we found that separate MFs and AFs per neuron are required to describe our monkey data, a result further supported by a model comparison analysis (Figure S5). Importantly, we found that multiplicative and additive effects are not randomly intermixed across neurons. Instead, neurons with strong modulation of one type tend to show weak modulation of the other. In addition, we found that the strength of spontaneous activity preceding stimulus onset induces not only an additive modulation of stimulus-evoked responses as described in previous work (Arieli et al., 1996), but also a multiplicative effect. However, the influence of pre-stimulus population activity on tuning was weaker than that of stimulus-evoked population activity fluctuations, presumably because activity fluctuations have a timescale of a few hundreds of milliseconds.

Several recent studies have addressed how network state affects sensory responses and encoding, generally defining states based on the degree to which activity is synchronized across neurons or based on LFP measurements (Luczak et al., 2013; Mochol et al., 2015; Pachitariu et al., 2015; Schölvinck et al., 2015). In these works, it is often reported that correlations are coupled with population activity measurements (Mochol et al.,

2015; Pachitariu et al., 2015; Schölvinck et al., 2015). Much less attention has been paid, however, to the question of how within-state, across-trials fluctuations in the strength of population activity affect neuronal tuning and encoded information, although these fluctuations have been well documented (Arieli et al., 1996; Kenet et al., 2003; Tsodyks et al., 1999). In our data, fluctuations of population activity strength do not correspond to changes in the degree of network synchronization because neither variability nor correlations change substantially when going from low to high population activity (Figure S6). This may be because fluctuations of population activity in our data correspond to within-state fluctuations, rather than to across-state fluctuations. In fact, our analysis shows that the distributions of population activity are unimodal, suggesting a single state (Figures 2A and S2A). Overall, by performing an analysis in which population activity was the central quantity to condition on, we were able to reveal that across-trials fluctuations in the strength of population activity affect sensory tuning and the information encoded in distinct subsets of neurons.

Interestingly, our results show that the multiplicative effects on orientation tuning are as large in the awake animal as in the anesthetized preparation. This similarity in modulation occurred despite differences in the magnitude of pairwise correlations between our datasets from awake and anesthetized animals (median pairwise spike count correlations in 160- to 260-ms window for anesthetized data: $\rho = 0.073$, D1; $\rho = 0.091$, D2; $\rho = 0.043$, D3; $\rho = 0.061$, D4; and for awake: $\rho = 0.013$, D5). However, the smaller pairwise correlations observed in the awake preparation nevertheless involved substantial shared fluctuation in the full population, which were clearly evident when we conditioned on the population activity of ~ 20 units. Therefore, although the magnitude of pairwise correlations might vary across experimental preparations (e.g., brain state, cortical areas, layers) (Cohen and Kohn, 2011; Ecker et al., 2010, 2014; Kohn and Smith, 2005), their net effect on the population can be similar. Indeed, recent work has emphasized that the magnitude of pairwise correlations is not informative about their functional impact; even tiny correlations of a particular form called differential correlations can have massive effects on population information, whereas large correlations with a different structure can have little effect (Moreno-Bote et al., 2014).

A modulation of sensory tuning similar to the one that we report has been observed with optogenetic stimulation of specific V1 neuronal subpopulations. Optogenetic stimulation of layer 6 in mouse primary visual cortex induces divisive (i.e., multiplicative) gain modulation of orientation-selective neurons in the upper layers (Olsen et al., 2012). Similarly, optogenetic stimulation of inhibitory neurons in rat primary visual cortex has been shown to cause divisive or subtractive changes in the tuning of target neurons, depending on the inhibitory subpopulation that is stimulated (Wilson et al., 2012). More recently, antidromic spikes generated by optogenetic stimulation of distal V1 locations have been shown to additively and divisively modulate layer 2/3 neuronal responses in the mouse (Sato et al., 2014). These effects are similar to those we report, although future work will need to determine whether they provide a mechanistic explanation for the effects we observe under stimulus-driven conditions. An alternative explanation is that additive and multiplicative

modulation can arise from balanced excitatory and inhibitory inputs (Chance et al., 2002). Specifically, multiplicative modulation arises from excitatory and inhibitory currents that are tightly balanced, whereas additive modulation might involve a slight imbalance in these currents. In this context, our results suggest that the balance of excitation and inhibition varies across neurons.

One might be tempted to equate the modulation of single neuron activity that we observe to that induced by the allocation of attention. Indeed, attention has been shown to modulate tuning in multiplicative and additive manners, similar to the modulation of tuning that what we have observed with population activity (Baruni et al., 2015; McAdams and Maunsell, 1999; Thiele et al., 2009; Treue and Martínez Trujillo, 1999). However, attention has been also shown to reduce response variability and pairwise correlations (Cohen and Maunsell, 2009; Mitchell et al., 2009) (but see Ruff and Cohen, 2014), whereas we found little change in these measures with fluctuations in population activity (Figure S6). Multiplicative modulation of tuning is also evident with manipulations of stimulus contrast (Carandini and Heeger, 1994; Finn et al., 2007; Priebe and Ferster, 2012). It is possible that the multiplicative modulation of tuning we report here shares similar mechanisms to those that occur with manipulations of stimulus contrast. In this regard, it is worth noting that the similarity of the multiplicative modulation we report to variations caused by altering contrast suggests that fluctuations in population activity limit information about stimulus contrast in V1, perhaps explaining limitations on perceptual contrast discriminability. This is because fluctuations that are identical to those generated by stimulus variations are the ones that limit information about the stimulus (Moreno-Bote et al., 2014).

The neuron-specific modulation of tuning with population activity fluctuations that we have characterized might govern important aspects of sensory processing, as these fluctuations affect the amount of sensory information that can be read out from small neuronal ensembles. For instance, the modulation might contribute to the trafficking of information in primary visual cortex because an increase in overall activity tends to boost information in multiplicatively modulated neurons while impoverishing it in additively modulated neurons. Although we have shown that population activity does not substantially change total information in the recorded population, population activity through its neuron-specific multiplicative and additive modulations may act as a global context or traffic light, which influences which neuronal ensembles convey more information about the stimulus. In a speculative vein, efficient synaptic plasticity in small neuronal assemblies requires that their responses carry information about relevant internal and external variables (Fusi et al., 2007; Urbanczik and Senn, 2009), so modulating their information about those variables can also gate plasticity. Therefore, population activity might also control important aspects of learning.

EXPERIMENTAL PROCEDURES

Animal Preparation

We recorded data from five adult male macaque monkeys (*Macaca fascicularis*), four anesthetized and one performing a fixation task. The techniques used

in anesthetized animals have been previously described (Smith and Kohn, 2008). Briefly, anesthesia was induced with ketamine (10 mg/kg) and maintained during preparatory surgery with isoflurane (1.5%–2.5% in 95% O₂). Sufentanil citrate (6–24 μg/kg/hr, adjusted as needed for each animal) was used to maintain anesthesia during recordings (see Supplemental Experimental Procedures).

For experiments involving the awake monkey, the animal was implanted with a head post and then trained to fixate in a 1-degree window. Eye position was monitored with a high-speed infrared camera (Eyelink, 1,000 Hz). At 500 ms after the establishment of fixation, a drifting grating appeared over the aggregate receptive field of the recorded units. If the animal broke fixation, the trial was aborted and the data discarded. The animal was rewarded with a drop of water for successfully completed trials, typically ~500–800 per session.

All procedures were approved by the Institutional Animal Care and Use Committee of the Albert Einstein College of Medicine at Yeshiva University and were in compliance with the guidelines set forth in the United States Public Health Service Guide for the Care and Use of Laboratory Animals.

Visual Stimuli

For anesthetized animals, we presented full contrast drifting sinusoidal grating for 1,280 ms, with an interstimulus period of 1,500 ms. Gratings of eight different orientation were each shown 300–400 times. For the awake animal, we used 12 different orientations, and each was presented for 350 ms, with an interstimulus period of 50 ms. After every four stimuli, the monkey was rewarded. We recorded 50 trials for each stimulus orientation (see Supplemental Experimental Procedures).

Recording Methods and Data Preprocessing

We recorded in the superficial layers of primary visual cortex (V1), using a Utah array (96 microelectrodes, 1-mm length, 400-μm spacing; 48 electrodes in the awake animal). Events crossing a user-defined threshold were digitized (30 kHz), saved, and sorted offline. We quantified spike waveform quality using a simple signal-to-noise ratio metric (SNR; Kelly et al., 2007). We defined multiunits (MUA) to be units with SNR > 2, which corresponds to clusters with a small number of single units. Well-isolated units were defined to have SNR > 3.5, a conservative threshold. A small number of MUA sites with SNR < 2 were also used only to compute the population activity.

We only analyzed blocks of trials in which responses did not change markedly over time. While the data from anesthetized animals were quite stable, those from the awake preparation showed strong evidence of adaptation. We therefore removed from this dataset the first 200 trials, leaving 400 trials during which responses were stable. To avoid biases due to a different number of trials per orientation in the decoding performance analysis, we (randomly) selected 30 trials for each orientation. Because of the low number of trials compared with the “anesthetized” datasets, we merged trials with adjacent orientations in pairs to obtain six orientations with 60 trials per orientation to offer more comparable results. For all datasets, we measured responses beginning 60 ms after stimulus onset to account for V1 response latencies, as in Graf et al. (2011).

Dependence of Tuning Curves on Population Activity

Tuning conditioned to population activity was computed for every orientation-selective unit using the following model-free approach. Orientation-selective neurons were defined as those with tuning well fitted by a von Mises function ($r^2 \geq 0.75$) (Graf et al., 2011); remaining neurons were termed non-selective. For each trial, we computed the population activity as the average number of spikes per second across all other neurons in that time window. Population activity was based on *all* neurons except the one for which tuning modulation was computed. Trials corresponding to a given stimulus orientation were sorted as a function of mean population activity and then split at their median into subgroups of “low” and “high” activity. We computed the high and low population activity tuning, denoted $f^{high}(\theta)$ and $f^{low}(\theta)$, as the firing rate of the chosen neuron as a function of stimulus orientation in trial subgroups with high and low population activity, respectively. For comparison, we also computed population activity after Z scoring the responses of each neuron across trials. This approach yielded similar results because trial ranking was

nearly identical with the two methods, with only a few close-to-median trials changing category.

Multiplicative and Additive Modulation of Tuning

To estimate the multiplicative and additive gains, we performed a type II weighted linear regression between the low and high tuning, using the model $f^{high}(\theta) = g f^{low}(\theta) + s$, where g is the MF and s is an additive offset. The MF is unit-less by definition. To obtain a comparable unit-less AF, we normalized s by the mean activity across orientations. Neurons with fit values outside the range (0.3, 3) for MFs and (-1, 1) for AFs were excluded from analysis. Results do not qualitatively depend on the exclusion of these few outliers (5% of cases).

For each dataset, we estimated the gains' significance by a permutation test that sampled the null hypothesis. We randomly assigned trials to build high and low tuning, instead of ranking trials by population activity. Then we obtained the MFs and AFs for each neuron by linear regression, as described before, and computed the median factors across all neurons. We repeated this procedure 1,000 times. We defined the probability that these medians were larger or smaller than the real median across neurons by the fraction of samples below or above the real population median. The reported two-tailed p values were twice that fraction.

The statistical analysis for the correlation between MFs and AFs (Figure 3D) is described in the [Supplemental Experimental Procedures](#).

Broadening and Displacement of Tuning Curves

We determined the change in width and preferred orientation with population activity using Von Mises function fits to each neuron: $f(\theta) = a + b \exp[k * [\cos(2 * (\theta - \theta_{pref})) - 1]]$, for trials with low and high population activity. We fit the function by minimizing the weighted squared error with bounded parameters to ensure physiologically plausible parameters (minimize function from `lmfit` python package with the following constraints: $\theta \in [0, \pi]$, $k > 0.001$, $\max(f_{\theta}) < 1.3 * \max(\bar{f}_{\theta})$, $\min(f_{\theta}) > 0.7 * \min(\bar{f}_{\theta})$, where \bar{f}_{θ} is the mean response across trials for each orientation). To evaluate broadening, we used the squared width of the von Mises distribution, defined as $\sigma^2 = 1 - I_1(k)/I_0(k)$, where $I_n(k)$ is the modified Bessel function of the first kind of order n evaluated at k . The *broadening factor* was computed as the ratio between the widths of the high and low tuning ($\sigma^{high}/\sigma^{low}$). The *displacement* of the tuning was defined as the absolute difference between the preferred orientation of the high and low tuning ($\Delta\theta_{pref} = |\theta_{pref}^{high} - \theta_{pref}^{low}|$). We tested for significant broadening and displacement with a permutation test by sampling, as described above, using two-tailed and one-tailed p values, respectively. In an additional analysis, we used the von Mises fits to compute the multiplicative and additive modulation of tuning, which yielded similar results to those reported in the main text.

Extracting Visual Information from Population Recordings

We defined decoding performance (Figures 5, 6, and 7) as the fraction of trials where stimulus orientation was correctly predicted by a trained decoder. Results shown are for multinomial logistic regression (MLR) (Bishop, 2006) (see [Supplemental Experimental Procedures](#)), which outperformed a linear SVM decoder (an obvious alternative). We used 10-fold cross-validation (CV) to avoid over fitting the data; reported performance is the average performance across the ten sets of left-out data.

Decoding Performance as a Function of Population Activity

We computed the decoding performance in the time window 160–260 ms after stimulus onset using simultaneously recorded small ensembles of $N = 1, 2, 3, 5, 10, \text{ or } 15$ neurons. Decoding performance was independently analyzed for each orientation and each ensemble (Figure 7) using MLR with the population vector formed by the firing rates of the neurons of the ensemble. Trials for each orientation were divided into low and high population activity trials, and their averages across trials were computed (Figure 5). As for the tuning analysis, population activity was computed using all neurons but excluding the N neurons of the ensemble. Performance change per orientation was defined as the difference in decoding performance between high and low population activity trials for the MLR decoder trained in the two conditions and across orientations. We report the Pearson correlation coefficient and its two-tailed

p value, and we also plot a linear regression to highlight the relationship between performance change and mean factors in the ensemble.

SUPPLEMENTAL INFORMATION

Supplemental Information includes Supplemental Experimental Procedures and seven figures and can be found with this article online at <http://dx.doi.org/10.1016/j.neuron.2016.01.044>.

AUTHOR CONTRIBUTIONS

I.A.-R., J.D., and R.M.-B. conceived the research. S.T. and A.K. collected the data. I.A.-R. analyzed the data and generated results and figures. All authors discussed results and wrote the paper.

ACKNOWLEDGMENTS

I.A.-R. is supported by a PhD grant from the Department of Education, Linguistic Politics, and Culture of the Basque Government. A.K. is supported by the NIH (EY016774), an Irma T. Hirsch Career Scientist Award, and Research to Prevent Blindness. R.M.-B. is supported by the Ramón y Cajal Spanish Award RYC-2010-05952, the Marie Curie FP7-PEOPLE-2010-IRG grant PIRG08-GA-2010-276795, and the Spanish PSI2013-44811-P grant. I.A.-R. thanks A. Pouget for his hospitality at the University of Geneva.

Received: April 7, 2015

Revised: December 9, 2015

Accepted: January 16, 2016

Published: February 25, 2016

REFERENCES

- Arieli, A., Sterkin, A., Grinvald, A., and Aertsen, A. (1996). Dynamics of ongoing activity: explanation of the large variability in evoked cortical responses. *Science* 273, 1868–1871.
- Averbeck, B.B., Latham, P.E., and Pouget, A. (2006). Neural correlations, population coding and computation. *Nat. Rev. Neurosci.* 7, 358–366.
- Baruni, J.K., Lau, B., and Salzman, C.D. (2015). Reward expectation differentially modulates attentional behavior and activity in visual area V4. *Nat. Neurosci.* 18, 1656–1663.
- Bishop, C.M. (2006). *Pattern Recognition and Machine Learning* (Singapore: Springer).
- Carandini, M., and Heeger, D.J. (1994). Summation and division by neurons in primate visual cortex. *Science* 264, 1333–1336.
- Chance, F.S., Abbott, L.F., and Reyes, A.D. (2002). Gain modulation from background synaptic input. *Neuron* 35, 773–782.
- Cohen, M.R., and Kohn, A. (2011). Measuring and interpreting neuronal correlations. *Nat. Neurosci.* 14, 811–819.
- Cohen, M.R., and Maunsell, J.H. (2009). Attention improves performance primarily by reducing interneuronal correlations. *Nat. Neurosci.* 12, 1594–1600.
- Ecker, A.S., Berens, P., Keliris, G.A., Bethge, M., Logothetis, N.K., and Tolias, A.S. (2010). Decorrelated neuronal firing in cortical microcircuits. *Science* 327, 584–587.
- Ecker, A.S., Berens, P., Cotton, R.J., Subramanian, M., Denfield, G.H., Cadwell, C.R., Smirnakis, S.M., Bethge, M., and Tolias, A.S. (2014). State dependence of noise correlations in macaque primary visual cortex. *Neuron* 82, 235–248.
- Finn, I.M., Priebe, N.J., and Ferster, D. (2007). The emergence of contrast-invariant orientation tuning in simple cells of cat visual cortex. *Neuron* 54, 137–152.
- Fiser, J., Chiu, C., and Weliky, M. (2004). Small modulation of ongoing cortical dynamics by sensory input during natural vision. *Nature* 431, 573–578.

- Fusi, S., Asaad, W.F., Miller, E.K., and Wang, X.J. (2007). A neural circuit model of flexible sensorimotor mapping: learning and forgetting on multiple time-scales. *Neuron* 54, 319–333.
- Goris, R.L., Movshon, J.A., and Simoncelli, E.P. (2014). Partitioning neuronal variability. *Nat. Neurosci.* 17, 858–865.
- Graf, A.B., Kohn, A., Jazayeri, M., and Movshon, J.A. (2011). Decoding the activity of neuronal populations in macaque primary visual cortex. *Nat. Neurosci.* 14, 239–245.
- Kelly, R.C., Smith, M.A., Samonds, J.M., Kohn, A., Bonds, A.B., Movshon, J.A., and Lee, T.S. (2007). Comparison of recordings from microelectrode arrays and single electrodes in the visual cortex. *J. Neurosci.* 27, 261–264.
- Kenet, T., Bibitchkov, D., Tsodyks, M., Grinvald, A., and Arieli, A. (2003). Spontaneously emerging cortical representations of visual attributes. *Nature* 425, 954–956.
- Kohn, A., and Smith, M.A. (2005). Stimulus dependence of neuronal correlation in primary visual cortex of the macaque. *J. Neurosci.* 25, 3661–3673.
- Lin, I.C., Okun, M., Carandini, M., and Harris, K.D. (2015). The Nature of Shared Cortical Variability. *Neuron* 87, 644–656.
- Luczak, A., Bartho, P., and Harris, K.D. (2013). Gating of sensory input by spontaneous cortical activity. *J. Neurosci.* 33, 1684–1695.
- Ma, W.J., Beck, J.M., Latham, P.E., and Pouget, A. (2006). Bayesian inference with probabilistic population codes. *Nat. Neurosci.* 9, 1432–1438.
- McAdams, C.J., and Maunsell, J.H. (1999). Effects of attention on orientation-tuning functions of single neurons in macaque cortical area V4. *J. Neurosci.* 19, 431–441.
- Mitchell, J.F., Sundberg, K.A., and Reynolds, J.H. (2009). Spatial attention decorrelates intrinsic activity fluctuations in macaque area V4. *Neuron* 63, 879–888.
- Mochol, G., Hermoso-Mendizabal, A., Sakata, S., Harris, K.D., and de la Rocha, J. (2015). Stochastic transitions into silence cause noise correlations in cortical circuits. *Proc. Natl. Acad. Sci. USA* 112, 3529–3534.
- Moreno-Bote, R., Beck, J., Kanitscheider, I., Pitkow, X., Latham, P., and Pouget, A. (2014). Information-limiting correlations. *Nat. Neurosci.* 17, 1410–1417.
- Okun, M., Steinmetz, N.A., Cossell, L., Iacaruso, M.F., Ko, H., Barthó, P., Moore, T., Hofer, S.B., Mscic-Flogel, T.D., Carandini, M., and Harris, K.D. (2015). Diverse coupling of neurons to populations in sensory cortex. *Nature* 521, 511–515.
- Olsen, S.R., Bortone, D.S., Adesnik, H., and Scanziani, M. (2012). Gain control by layer six in cortical circuits of vision. *Nature* 483, 47–52.
- Pachitariu, M., Lyamzin, D.R., Sahani, M., and Lesica, N.A. (2015). State-dependent population coding in primary auditory cortex. *J. Neurosci.* 35, 2058–2073.
- Priebe, N.J., and Ferster, D. (2012). Mechanisms of neuronal computation in mammalian visual cortex. *Neuron* 75, 194–208.
- Ruff, D.A., and Cohen, M.R. (2014). Attention can either increase or decrease spike count correlations in visual cortex. *Nat. Neurosci.* 17, 1591–1597.
- Sato, T.K., Häusser, M., and Carandini, M. (2014). Distal connectivity causes summation and division across mouse visual cortex. *Nat. Neurosci.* 17, 30–32.
- Schölvinck, M.L., Saleem, A.B., Benucci, A., Harris, K.D., and Carandini, M. (2015). Cortical state determines global variability and correlations in visual cortex. *J. Neurosci.* 35, 170–178.
- Seung, H.S., and Sompolinsky, H. (1993). Simple models for reading neuronal population codes. *Proc. Natl. Acad. Sci. USA* 90, 10749–10753.
- Shadlen, M.N., and Newsome, W.T. (1998). The variable discharge of cortical neurons: implications for connectivity, computation, and information coding. *J. Neurosci.* 18, 3870–3896.
- Smith, M.A., and Kohn, A. (2008). Spatial and temporal scales of neuronal correlation in primary visual cortex. *J. Neurosci.* 28, 12591–12603.
- Thiele, A., Pooresmaeili, A., Delicato, L.S., Herrero, J.L., and Roelfsema, P.R. (2009). Additive effects of attention and stimulus contrast in primary visual cortex. *Cereb. Cortex* 19, 2970–2981.
- Tolhurst, D.J., Movshon, J.A., and Dean, A.F. (1983). The statistical reliability of signals in single neurons in cat and monkey visual cortex. *Vision Res.* 23, 775–785.
- Treue, S., and Martínez Trujillo, J.C. (1999). Feature-based attention influences motion processing gain in macaque visual cortex. *Nature* 399, 575–579.
- Tsodyks, M., Kenet, T., Grinvald, A., and Arieli, A. (1999). Linking spontaneous activity of single cortical neurons and the underlying functional architecture. *Science* 286, 1943–1946.
- Urbanczik, R., and Senn, W. (2009). Reinforcement learning in populations of spiking neurons. *Nat. Neurosci.* 12, 250–252.
- Wilson, N.R., Runyan, C.A., Wang, F.L., and Sur, M. (2012). Division and subtraction by distinct cortical inhibitory networks in vivo. *Nature* 488, 343–348.